

Toward Network Electrochromic Film: Secondary Polymerization of Methacrylate Functionalized Thiophene

Shouli Ming¹‡, Shimin Zhang²‡, Hongtao Liu¹, Zhipeng Wang¹, Yao Zhao¹ and Jingkun Xu^{1,*}

¹ Jiangxi Key Laboratory of Organic Chemistry, Jiangxi Science and Technology Normal University, Nanchang 330013, China

² Academy of Fundamental and Interdisciplinary Sciences, Harbin Institute of Technology, Harbin, 150001, China

*E-mail: xujingkun@tsinghua.org.cn

‡: These authors contributed equally to this work.

Received: 22 May 2015 / Accepted: 28 June 2015 / Published: 28 July 2015

A novel methacrylate modified 2-(3-thienyl)ethyl methacrylate (TE-MA) was synthesized, and free radical polymerized and electrochemical polymerized to obtain the precursor polymer polymethacrylate (PMA) functionalized with thiophene (TE-PMA) and PMA modified polythiophene (PTE-PMA), respectively. Structure characterization and properties of PTE-PMA, including FT-IR, morphology, electrochemical, and electrochromic properties, were systematically investigated. In addition, PTE-PMA exhibited obvious color changes from gray to purple and good electrochromic properties, including satisfactory coloration efficiency ($128 \text{ cm}^2 \text{ C}^{-1}$ at 400 nm; $115 \text{ cm}^2 \text{ C}^{-1}$ at 900 nm) and fast response time.

Keywords: conducting polymer, polythiophene, network, electrochemical polymerization, electrochromics

1. INTRODUCTION

Electrochromics change the absorption band of the materials through charge injection and removal [1,2]. In particular, conducting polymer have been regarded as potential electrochromes in optical displays, smart windows and electrochromic camouflages due to their advantages compared to inorganic materials including multicolor with one conjugated polymer, ease process of organic electrochromic materials with the large surfaces, high optical and electrochemical stability, and high optical contrast ratio with low response time [1-8]. Based on this, the design and synthesis of novel electrochromic polymer is highly necessary.

As is known to all scientists in electrochromic field, polythiophenes are the most extensively explored in electrochromic field. The unsubstituted polythiophene revealed obvious color change from red to blue attributing to the change of π - π^* transition with simultaneous formation of polaron in near-infrared region [9,10]. In the context of electrochromism, considering lower potentials of oligomers, bithiophene has been polymerized by electrochemical method. And the polythiophene from bithiophene was red on neutral state, light blue on oxidized state, and dark blue on reduced state, which was different from that of polythiophene from thiophene [11,12]. Considering the ease of functionalization and structure-controlled optical properties, since then polythiophenes have attracted lots of attention as electrochromic materials.

In particular, substituents not only change the redox potential, solubility and band gap of the polymer, but modify the electrochromic performance through sterically hindering and pull-push dual-effect of substituents [13-22]. Methacrylate is regarded as a popular crosslinking and sterilizing group. Previously reported acrylate/methacrylate modified ProDOTs and PEDOTs were regarded as photopatterning electrochromic materials for the fabrication of devices [13-15]. Interestingly, the network film exhibited enhanced stability compared to corresponding chainlike film [13], which has been demonstrated by Sotzing's work. For the commercialization of electrochromic polymer, long-term stability is essential factor.

Therefore, the methacrylate group was introduced into thiophene ring to obtain a precursor (TE-MA), and the precursor polymer (TE-PMA) was free radical polymerized. Finally, PMA modified polythiophene (PTE-PMA) with network was electrochemical polymerized, as shown in Scheme 1. In addition, the properties of PTE-PMA, including FT-IR, morphology, electrochemical, spectroelectrochemical and electrochromic properties, were systematically explored.

2. EXPERIMENTAL SECTION

2.1 Chemical

3-Thienylethanol (TE, 98%; J&K Scientific Ltd.) and Azodiisobutyronitrile (AIBN, 99%; Energy Chemical) were used directly without further purification. Dichloromethane (CH_2Cl_2 , analytical grade; Shanghai Vita Chemical Reagent Co., Ltd.), tetrahydrofuran (THF, analytical grade; Xilong Chemical) and boron trifluoride diethyl etherate (BFEE, J&K Scientific Ltd.) were refluxed and distilled under a nitrogen atmosphere before use. Tetrabutylammonium hexafluorophosphate (Bu_4NPF_6 , 99%; Energy Chemical) was dried under vacuum at 60 °C for 24 h before use. Other materials (analytical grade, >98%) were purchased from Shanghai Vita Chemical Reagent Co., Ltd. and were used directly without any further treatment.

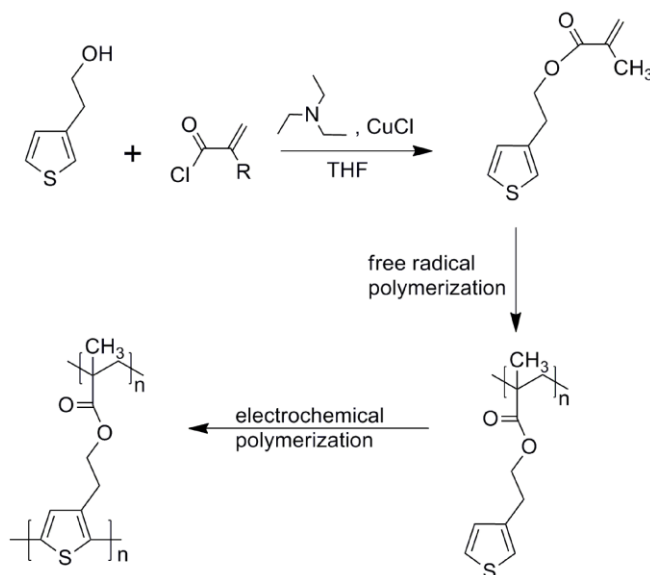
2.2 Characterization

^1H NMR and ^{13}C NMR spectra were measured by a Bruker AV 400 NMR spectrometer with CDCl_3 as the solvent and tetramethylsilane as an internal standard. Infrared spectra were recorded with a Bruker Vertex 70 Fourier-transform Infrared (FT-IR) spectrometer with samples in KBr pellets.

Scanning electron microscopy (SEM) image was performed on a VEGA II-LSU scanning electron microscope (Tescan).

2.3 Monomer synthesis

The monomers, 2-(3-thienyl)ethyl methacrylate (TE-MA) and poly[2-(3-thienyl)ethyl methacrylate] (TE-PMA), were prepared by the synthetic route in Scheme 1[17].



Scheme 1. Synthesis route for TE-MA, TE-PMA and PTE-PMA.

2-(3-Thienyl)ethyl methacrylate (TE-MA). The solution of 3-thiophenylethanol (5 g, 39.1 mmol), methacryloyl chloride (4.15 g, 39.68 mmol), dry triethylamine (5.6 g, 55.5 mmol) in THF (30 mL) and a small amount of CuCl were added to a flask. The solution was refluxed at 70 °C for 8 h under a nitrogen atmosphere. The resulting mixture was poured into water and extracted with CH₂Cl₂. The organic layer was washed with water, dried with MgSO₄ and removed by rotary evaporation. Finally, the product was purified by silica column chromatography to obtain 3.9 g colourless liquid. (Yield: 65%) ¹H NMR (400 MHz, CDCl₃): δ (ppm) 7.28 (m, 1H), 6.98-7.04 (m, 2H), 6.09 (t, 1H), 5.56 (t, 1H), 4.37 (t, 2H), 3.02 (t, 2H), 1.94 (s, 3H). ¹³C NMR (100 MHz, CDCl₃): δ (ppm) 167.2, 138.1, 136.2, 128.2, 125.5, 121.5, 64.5, 29.5, 18.3.

Poly[2-(3-thienyl)ethyl methacrylate] (TE-PMA). TE-PMA was prepared by free-radical polymerization with azobisisobutyronitrile (AIBN) as the initiator. After TE-MA was consumed, the reaction mixture was added into soxhlet thimble, washed with methanol and dried in vacuum. Finally, the product was purified by repeated precipitations to obtain white solid. ¹H NMR (400 MHz, CDCl₃): δ (ppm) 7.26 (s, 1H), 6.94-7.01 (b, 2H), 4.14 (b, 2H), 2.94 (b, 2H), 1.75-1.82 (b, 2H), 0.76-0.87 (b, 3H). GPC: M_n = 24837, M_w = 101574, M_w/M_n = 4.09.

2.4 Electrosynthesis and electrochemical test

Electrochemical tests were performed in self-assembly electrolytic cell by a Model 263A potentiostat-galvanostat (EG&G Princeton Applied Research). The electrolytic cell contains an Ag/AgCl reference electrode and two Pt wires as the working electrode and the counter electrode, respectively. To get sufficient polymer, Pt wires were replaced by Pt sheets as the work electrode and the counter electrode. During the electrochemical examinations, the two Pt sheets were placed 5 mm apart., Except for reference electrode, these electrodes were polished and cleaned carefully prior to each experiment. To remove the electrolyte, monomers, and oligomers, the polymer attached to Pt sheet was washed repeatedly with anhydrous CH₂Cl₂. Besides, the solvent-electrolyte systems were blanked by nitrogen stream before each experiment.

2.5 Electrochromic Test

Electrochromic properties were recorded on a Cary 50 Ultraviolet-Visible Near-Infrared spectrophotometer. The electrolytic cell includes ITO-coated glass as the working electrode, a Pt wire counter electrode, an Ag/AgCl reference electrode and a transparent cuvette used as the container. All electrochromic tests were performed in CH₂Cl₂-Bu₄NPF₆ (0.1 mol L⁻¹). It should be noted here that the solvent-electrolyte systems were blanked by nitrogen stream before each experiment.

On the basis of the following equations, the optical density (ΔOD) and the coloration efficiency (CE) are calculated [1,23,24]:

$$\Delta OD = \log(T_{\text{ox}}/T_{\text{red}}) \quad (1)$$

$$CE = \Delta OD/Q_d \quad (2)$$

where T_{ox} and T_{red} are transmittance of electrochromic material at oxidized and reduced states. Q_d is injected/ejected charge of electrochromic material in per unit.

3. RESULTS AND DISCUSSION

3.1 Electrochemical polymerization

To choose the suitable solvent, the electrochemical polymerization performances of TE-PMA (1.84 g L⁻¹) were explored by cyclic voltammetry (CV) in BFEE, CH₂Cl₂-BFEE (1:4, by volume) and CH₂Cl₂-BFEE (1:1, by volume). CV of TE-PMA was directly studied in BFEE, as shown in Figure 1A. CVs of TE-PMA in this medium revealed no obvious redox peaks, which was attributed to the poor solubility of TE-PMA in BFEE. In addition, there was no PTE-PMA attached on the working electrode. Therefore, CH₂Cl₂ was added to the system, as shown in Figure 1B. The decrease of equilibrium concentration of TE-PMA results in a decrease of peak current after several cycles of CV scans. Combining the good solubility of TE-PMA in CH₂Cl₂ and the facile synthesis of high-quality polymer films in BFEE [25-27], a solvent electrolyte containing 50% (vol) BFEE and 50% (vol) CH₂Cl₂ was chosen as the electrolyte system (Figure 1C).

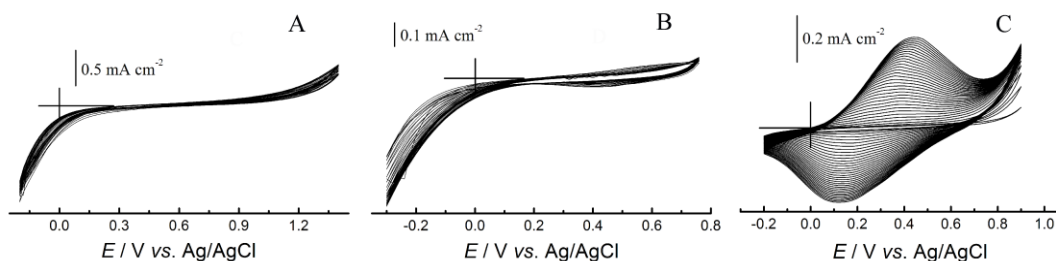


Figure 1. CVs of TE-PMA in BFEE (A), CH_2Cl_2 -BFEE (1:4, by volume) (B) and CH_2Cl_2 -BFEE (1:1, by volume) (C). Monomer concentration: 1.84 g L^{-1} . Scan rates: 100 mV s^{-1} .

The oxidation potential of TE-PMA (first cycle of Figure 1C) is found at 0.80 V , which is lower than that for its analog 3-thienylethanol (0.94 V). This indicated that the TE-PMA has a higher conjugated length [28,29]. During the repetitive anodic potential scan, the current intensities grew steadily. The phenomenon clearly demonstrated that PTE-MA attached on the work electrode grew. From the CV results, the corresponding polymer PTE-PMA exhibited broad redox waves. It could be ascribed to the formation of PTE-PMA with different chain length and the transition of conductive species [16]. And the oxidation and reduction peaks were observed at 0.44 and 0.12 V for PTE-PMA. During polymerization process, the peak potential change could be ascribed to the increased electrical resistance of PTE-PMA, and the resistance needed the over potential to overcome [26].

3.2 Optimization of electropolymerization condition

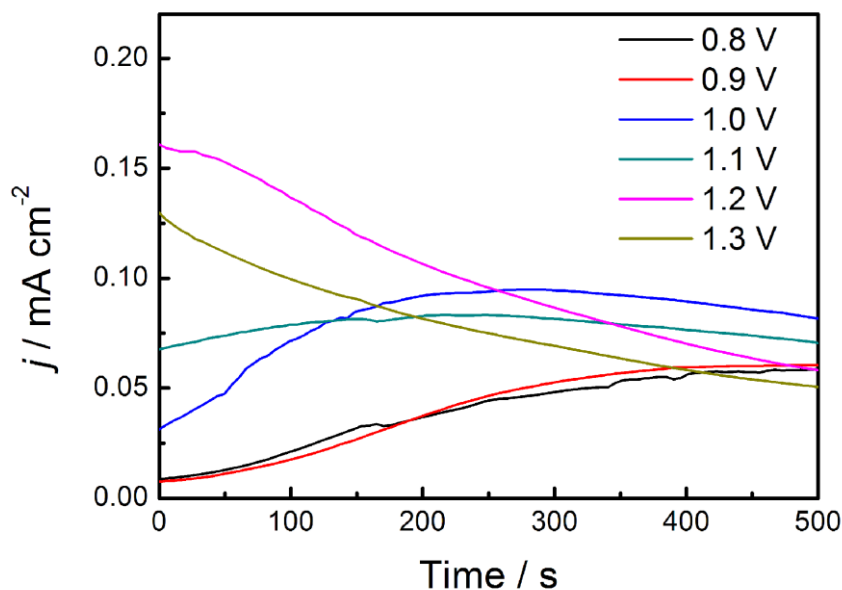


Figure 2. Chronoamperograms of TE-PMA in CH_2Cl_2 -BFEE (1:1, by volume) on the Pt electrode. Monomer concentration: 1.84 g L^{-1} .

The deposition potential significantly influences the structure and quality of polymer, which is in connection with various properties including stability and optical performance. In order to choose an appropriate potential for polymerization of TE-PMA, current density-time ($I-t$) curves of TE-PMA at 6 different potentials in CH_2Cl_2 -BFEE (1:1, by volume) were recorded, as shown in Figure 2. On the basis of chronoamperograms and phenomenon during the experiments, combining with the facts influence the quality of the polymer, the appropriate polymerized potential of TE-PMA was 1.1 V. Also, the continuous, homogeneous and smooth polymer film was obtained under optimized potential, in agreement with the $I-t$ curves.

3.3 Structural characterization

For conducting polymer, FT-IR spectrum is a very useful way to investigate the polymerized mechanism. As can be seen from Figure 3, FT-IR spectra of the monomer, polymerizable precursor (TE-PMA) and doped polymer (PTE-PMA) were recorded. FT-IR spectral peaks of PTE-PMA were broader relative to those of TE-MA and TE-PMA, in agreement with other reported conducting polymers. This mainly due to the presence of PTE-PMA with different length. The C=C stretching vibration frequency of the methacrylate transition at 1636 cm^{-1} appeared in TE-MA, and disappeared during free radical polymerization. The behavior demonstrated the formation of corresponding precursor polymer polymethacrylate. The peak at 3109 cm^{-1} for TE-MA (Figure 3A) was attributed to C-H vibration of the α -position of the thiophene unit. This peak was retained in TE-MA and TE-PMA (Figure 3) but disappeared in the electrochemical polymerized PTE-PMA (Figure 3C). It is obvious that the thiophene ring was not destroyed during the free radical polymerization of methacrylate and also that TE-PMA was polymerized to form PTE-PMA through α,α' -coupling of thiophene unit. The C=O vibration frequency for the ester group appeared as a large peak at 1716 cm^{-1} in both TE-MA, TE-PMA and PTE-PMA, with no obvious change in wavelength or intensity, demonstrating that the methacrylate unit was stable during the free radical polymerization and electropolymerization process.

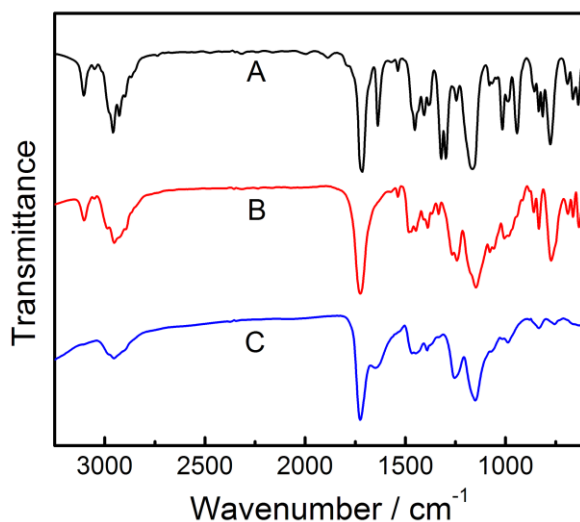


Figure 3. FT-IR spectra of TE-MA (A), TE-PMA (B) and PTE-PMA (C).

3.4 Electrochemistry of PTE-PMA film

To investigate the electrochemical activity and stability of obtained polymer, the electrochemical property of PTE-PMA film was performed in detail by cyclic voltammetry (CV) in monomer-free $\text{CH}_2\text{Cl}_2\text{-Bu}_4\text{NPF}_6$ (0.1 mol L^{-1}), as can be seen from Figure 4.

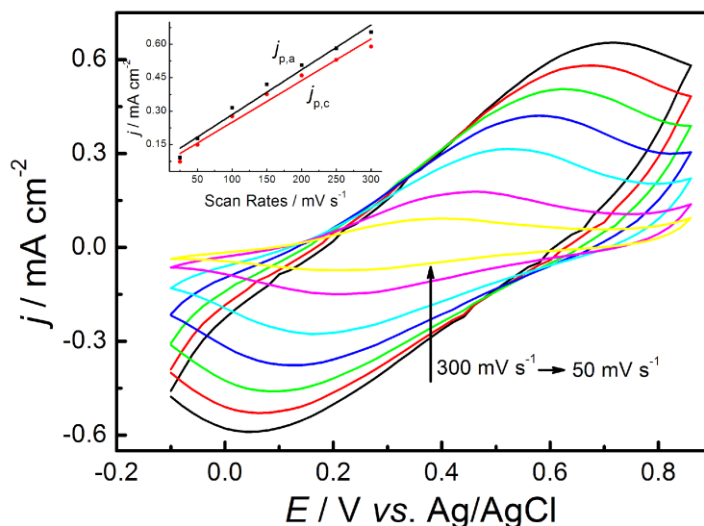


Figure 4. CVs of PTE-PMA in $\text{CH}_2\text{Cl}_2\text{-Bu}_4\text{NPF}_6$. Scan rates: $300 \sim 50 \text{ mV s}^{-1}$. Insert: plots of redox peak current densities vs. scan rates. $j_{p,a}$: the ratio between oxidized peak current densities and scan rates; $j_{p,c}$: the ratio between reduced peak current densities and scan rates.

The steady-state CVs of PTE-PMA revealed broad redox waves, which is consistent with CVs of TE-PMA. A true linear relation were observed between the scan rates and the peak current densities, which demonstrated that PTE-PMA was well attached to the electrode and the redox process was non-diffusional. Furthermore, the calculated $j_{p,a}/j_{p,c}$ ($j_{p,a}$: the ratio between oxidized peak current densities and scan rates; $j_{p,c}$: the ratio between reduced peak current densities and scan rates.) of PTE-PMA in $\text{CH}_2\text{Cl}_2\text{-Bu}_4\text{NPF}_6$ is closer to 1.0, indicating its better redox reversibility. There is a stark difference between the anodic and cathodic peak potentials in CV curves, which due to hysteresis effect during redox process. This phenomenon could be ascribed to a couple of reasons [26,27], including slow mutual transformation of various electronic species, slow heterogeneous electron transfer, rearrangement of polymer chains, and the transfer of interfacial electrons corresponding to the electrode/polymer and polymer/solution.

The electrochemical stability of active polymer is especially significant when considering the fabrication of electronic device. Therefore, the long-term redox stability of PTE-PMA was also investigated in $\text{CH}_2\text{Cl}_2\text{-Bu}_4\text{NPF}_6$ (0.1 mol L^{-1}), as shown in Figure 5. It was noted that PTE-PMA displayed good stability with the electrochemical activity still maintaining 81% after 1000 cycles. Even after 4000 cycles, the electrochemical activity of PTE-PMA still preserved up 69%. These results indicated good redox stability of PTE-PMA in comparison with polythiophene.

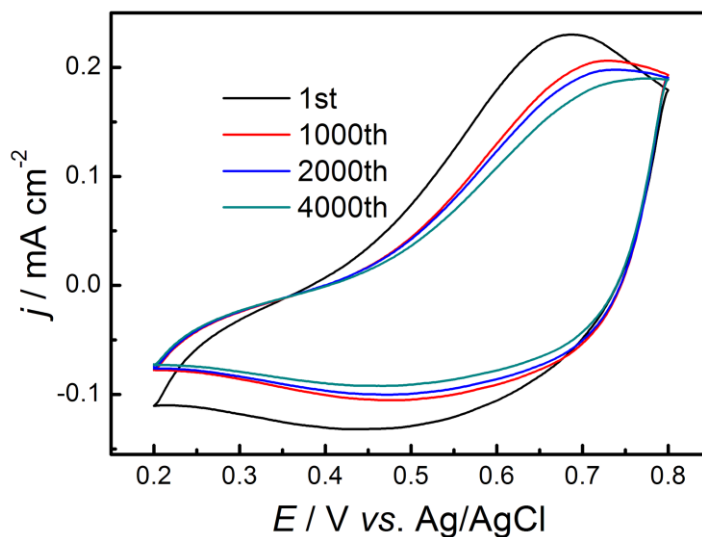


Figure 5. Cyclic voltammograms of PTE-PMA upon repeated cycling at the scan rate of 150 mV s^{-1} .

3.5 Morphology

To analyze the stability, electrical conductivity and redox activity of polymer, the surface morphology of PTE-PMA deposited on the ITO electrode was investigated by scanning electron microscopy (SEM), as shown in Figure 6. PTE-PMA film exhibited smooth and compact morphology at high magnifications, which was beneficial to increase the electrical conductivity of conjugated polymer. Also, the smooth and compact morphology of PTE-PMA was especially significant in fabrication of electrochromic device.

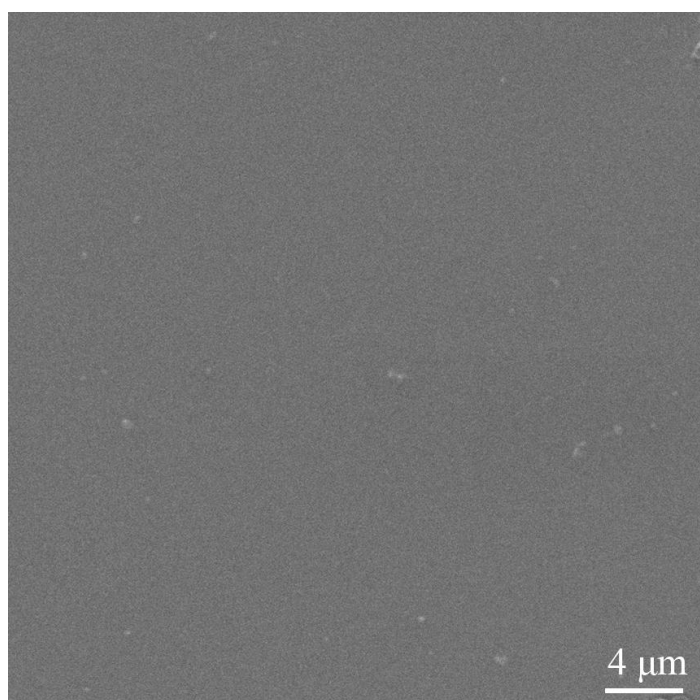


Figure 6. SEM images of PTE-PMA.

3.6 Spectroelectrochemical property

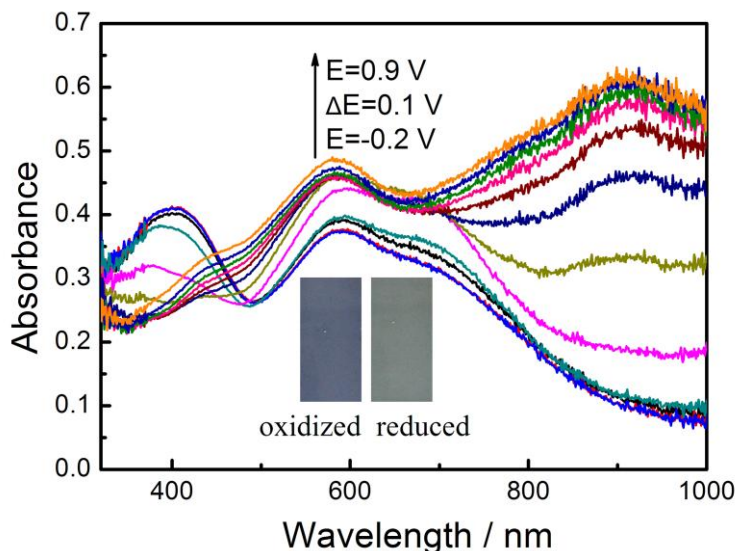


Figure 7. Spectroelectrochemistry and colors of PTE-PMA film on an ITO-coated glass in $\text{CH}_2\text{Cl}_2\text{-Bu}_4\text{NPF}_6$ (0.1 mol L^{-1}) at different applied potentials.

Spectroelectrochemical study of PTE-PMA film was performed in monomer-free $\text{CH}_2\text{Cl}_2\text{-Bu}_4\text{NPF}_6$ (0.1 mol L^{-1}) to evaluate electronic property and band gap (Figure 7). Thin PTE-PMA film was electrochemically deposited on transparent ITO-coated glass by potentiostatic method. In the reduced state, PTE-PMA revealed two absorption bands, centered at 400 nm and 580 nm, which was different from the absorption bands of PTE-MA. The absorption band at 400 nm originated from $\pi\text{-}\pi^*$ transition of thiophene ring, while the absorption band at 580 nm might due to free polymerized methacrylate [16]. Upon increase of potential applied to PTE-PMA, the intensities of the absorption band at 400 nm decreased, and the band at 580 nm and 900 nm began to intensify, which demonstrating that the formation of the polaron. At the same time, the color of PTE-PMA changed from grey to purple, corresponding to the spectrum change of PTE-PMA. In addition, the optical band gap of PTE-PMA was calculated on the basis of the formula $E_g = 1240/\lambda_{\text{onset}}$, where λ_{onset} is the onset of $\pi\text{-}\pi^*$ transition. The value of the optical bandgap for PTE-PMA was 2.58 eV.

3.7 Electrochromic property

The double step chronoamperometry method was used to monitor the transmittance changes between the neutral and the oxidized states upon optical switching of PTE-PMA, as shown in Figure 8. The electrochromic parameters of PTE-PMA, including optical contrast ratio (ΔT %), coloration efficiency, response time, and optical memory, were analyzed with the changes in transmittance. The potentials applied on PTE-PMA were changed alternatively between -0.2 V and 0.9 V for the switching time of 10 s. The electrochromic parameters of PTE-PMA are summarized in Table 1.

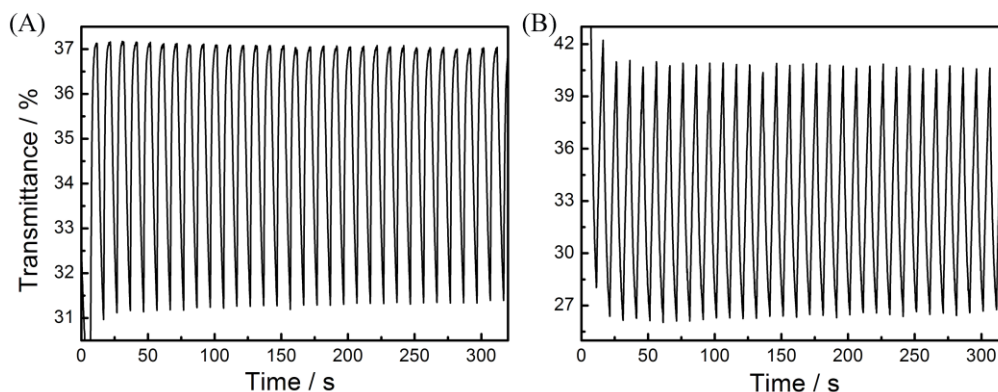


Figure 8. Transmittance monitored at 400 nm (A) and 900 nm (B) for PTE-PMA during double step spectrochronoamperometry between -0.2 V and 0.9 V. Switching time: 10 s.

The optical contrasts of PTE-PMA are 6% at 400 nm and 15% at 900 nm. Despite these values seem to be low, the color change was obvious during electrochromic switching process. Also, PTE-PMA switched rapidly and achieved 95% of its optical contrast in 2~5 s at all wavelengths. It was obvious that PTE-PMA had more fast response times at all wavelengths during oxidation process relative to reduction process (oxidation: 2.6 s at 400 nm, 4.3 s at 900 nm; reduction: 4.5 s at 400 nm, 4.6 s at 900 nm).

Table 1. Electrochromic parameters for PTE-PMA

polymer	Wavelength (nm)	$\Delta T/\%$	response time (s)		CE (cm^2/C)	λ (nm)		E_g (eV)
			oxidation	reduction		Abs. max	Abs. onset	
PTE-PMA	400	6	2.6	4.5	128	400	480	2.58
	900	15	4.3	4.6	115			

Coloration efficiency (CE), obtained for a certain amount of the charge inserted in the polymer as a function of the change in optical density, is also an important criterion for identifying the electrochromic performances [1]. In this work, CE of PTE-PMA were calculated as $128 \text{ cm}^2 \text{ C}^{-1}$ (at 400 nm) and $115 \text{ cm}^2 \text{ C}^{-1}$ (at 900 nm), respectively (Table 1).

4. CONCLUSIONS

In conclusion, a novel network polymer, PTE-PMA, was synthesized through two steps including free radical polymerization and electrochemical polymerization. Structure characterization and properties of PTE-PMA, including FT-IR, morphology, and electrochemical performance, were systematically explored. PTE-PMA revealed a obvious changes from gray to purple. In addition, PTE-

MA exhibited good electrochromic properties, including satisfactory coloration efficiency ($128 \text{ cm}^2 \text{ C}^{-1}$ at 400 nm; $115 \text{ cm}^2 \text{ C}^{-1}$ at 900 nm) and fast response time (2~5 s).

ACKNOWLEDGEMENTS

We are grateful to the National Natural Science Foundation of China (grant number: 51303073, 51463008), Ganpo Outstanding Talents 555 projects (2013), the Training Plan for the Main Subject of Academic Leaders of Jiangxi Province (2011), the Natural Science Foundation of Jiangxi Province (grant number: 20122BAB216011 and 20142BAB216029), the Science and Technology Landing Plan of Universities in Jiangxi province (KJLD12081), Provincial Projects for Postgraduate Innovation in Jiangxi (YC2014-S441, YC2014-S431), and National-level College Students' Innovation and Entrepreneurship Training Plan Program (2014QNBjrc003) for their financial support of this work.

References

1. P. M. Beaujuge and J. R. Reynolds, *Chem. Rev.*, 110 (2010) 268.
2. L. Groenendaal, G. Zotti, P. Aubert, S. M. Waybright and J. R. Reynolds, *Adv. Mater.*, 15 (2003) 855.
3. G. Gunbas and L. Toppare, *Chem. Commun.*, 48 (2012) 1083.
4. X. Wang, Y. Chen and X. Chen, *Prog. Chem.* 17 (2005) 451.
5. L. Beverina, G. A. Pagani and M. Sassi, *Chem. Commun.*, 50 (2014) 5413.
6. A.L. Dyer, M. R. Craig, J. E. Babiarz, K. Kiyak and J. R. Reynolds, *Macromolecules* 43 (2010) 4460.
7. C. G. Wu, M. I. Lu, S. J. Chang and C. S. Wei, *Adv. Funct. Mater.*, 17 (2007) 3153.
8. W. J. Doherty, R. J. Wysocki, N. R. Armstrong and S. R. Saavedra, *Macromolecules*, 39 (2006) 4418.
9. F. Garnier, G. Tourillon, M. Gazard and J. C. Dubois, *J. Electroanal. Chem.*, 148 (1983) 299.
10. M. A. Druy and R. J. Seymour, *Appl. Polym. Sci. Proc.*, 48 (1983) 561.
11. M. Aizawa, S. Watanabe, H. Shinohara and H. Shirakawa, *J. Chem. Soc., Chem. Commun.*, 5 (1985) 264.
12. F. Cecchet, C. A. Bignozzi, F. Paolucci and M. Marcaccio, *Synth. Met.*, 156 (2006) 27.
13. M. T. Otley, F. A. Alamer, Y. Zhu, A. Singhaviranon, X. Zhang, M. Li, A. Kumar, and G. A. Sotzing, *ACS Appl. Mater. Interfaces*, 6 (2014) 1734.
14. J. Kim, J. You and E. Kim, *Macromolecules*, 43 (2010) 2322.
15. J. Kim, J. You, B. Kim, T. Park and E. Kim, *Adv. Mater.*, 23 (2011) 4168.
16. L. Qin, J. Xu, B. Lu, Y. Lu, X. Duan and G. Nie, *J. Mater. Chem.*, 22 (2012) 18345.
17. M. L. Hallensleben, F. Hollwedel and D. Stanke, *Macromol. Chem. Phys.*, 196 (1995) 3535.
18. P. J. Costanzo and K. K. Stokes, *Macromolecules*, 35 (2002) 6804.
19. P. Camurlu, A. Cirpan and L. Toppare, *Synthetic. Met.*, 146 (2004) 91.
20. P. Camurlu, A. Cirpan and L. Toppare, *Mater. Chem. Phys.*, 92 (2005) 413.
21. H. B. Yildiz, S. Kiralp and L. Toppare, F. Yilmaz, Y. Yagci, K. Ito, T. Senyo, *Polym. Bull.*, 53 (2005) 193.
22. L. Sacan, A. Cirpan, P. Camurlu and L. Toppare, *Synthetic. Met.*, 156 (2006) 190.
23. C. L. Gaupp, D. M. Welsh, R. D. Rauh and J. R. Reynolds, *Chem. Mater.*, 14 (2002) 3964.
24. B. D. Reeves, C. R. G. Grenier, A. A. Argun, A. Cirpan, T. D. McCarley and J. R. Reynolds, *Macromolecules*, 37 (2004) 7559.
25. X. G. Li, M. R. Huang, W. Duan and Y. L. Yang, *Chem Rev*, 102 (2002) 2925.
26. W. Chen and G. Xue, *Prog. Polym. Sci.*, 30 (2005) 783-811.
27. G. W. Lu and G. Q. Shi, *J. Electroanal. Chem.*, 586 (2006) 154.

28. S. Zhen, X. Ma, B. Lu, S. Ming, K. Lin, L. Zhao, J. Xu and W. Zhou, *Int. J. Electrochem. Sci.*, 9 (2014) 7518.
29. B. Lu, L. Qin, W. Chen and J. Xu, *Int. J. Electrochem. Sci.*, 9 (2014) 4535.

© 2015 The Authors. Published by ESG (www.electrochemsci.org). This article is an open access article distributed under the terms and conditions of the Creative Commons Attribution license (<http://creativecommons.org/licenses/by/4.0/>).